

RESEARCH ARTICLE OPEN ACCESS

Valorization of Juice Industry Waste Into Foam-Like Materials Using Mycelium as Natural Binder

S. Najmeh Mousavi¹  | Paula Pou I Rodríguez² | Juliana Aristéia de Lima³ | E. R. Kanishka B. Wijayarathna¹  | Sunil Kumar Ramamoorthy¹  | Minna Hakkarainen²  | Akram Zamani¹

¹Swedish Center for Resource Recovery, University of Borås, Borås, Sweden | ²Department of Fiber and Polymer Technology, KTH Royal Institute of Technology, Stockholm, Sweden | ³Department of Polymer, Fibre and Composite, RISE Research Institutes of Sweden, Borås, Sweden

Correspondence: S. Najmeh Mousavi (Mousavi.nh@gmail.com) | Akram Zamani (akram.zamani@hb.se)

Received: 9 April 2025 | **Revised:** 20 January 2026 | **Accepted:** 10 March 2026

Keywords: *Aspergillus oryzae* | bubble column bioreactor | carrot pomace | cushioning and packaging | fungal biomass | mycelium-based foam | submerged cultivation

ABSTRACT

Growing environmental concerns associated with synthetic materials have intensified the demand for sustainable alternatives derived from renewable sources. In addition, the increasing global population has led to a surge in the demand for food products including juice, resulting in the generation of substantial quantities of byproducts, which are organic waste with the potential for valorization. This study investigated the bioconversion of carrot pomace (CP), waste generated in the juice industry, into fungal biomass to produce mycelium-based foams. Filamentous fungus (*Aspergillus oryzae*) was cultivated on carrot pomace through a submerged process in a bubble column bioreactor. The analysis of the scanning electron microscopy (SEM) confirmed the presence of the fungal mycelium and CP residues in the material recovered from the bioreactor. This material was mixed with water, and the suspension was subjected to different grinding cycles in an ultrafine grinder, and mycelium-based foams were then formed via freeze-molding and freeze-drying. The resulting foams exhibited an average density of 21.1 kg/m³, with compressive resistance values of 5.8 kPa at 10% deformation and 20.5 kPa at 30% deformation. These mechanical properties are comparable to those of commercial lightweight foams, as indicated by the Ashby material plot. These findings demonstrate the potential of mycelium-based foams as an alternative to synthetic materials, contributing to waste valorization and development of environmentally friendly materials.

1 | Introduction

Lightweight, three-dimensional porous structures are indispensable for various applications, including packaging, cushioning materials, acoustic and thermal insulation [1]. These structures are traditionally dominated by synthetic foams, such as polystyrene, polyolefin, and polyurethane, which are renowned for their versatility and performance. In 2022, the global market volume of polyurethane reached approximately 25.78 million metric tons, with projections indicating growth to 31.27 million metric tons by 2030 [2]. Similarly, global polystyrene production capacity was around 15.44 million

metric tons in 2022 and is expected to rise to 16.75 million metric tons by 2026, reflecting steady market expansion [3]. Despite their extensive use, these materials pose significant environmental and health concerns. One major issue is their non-biodegradability, leading to accumulation of microplastics in ecosystems, posing long-term ecological risks [4]. Moreover, the production and disposal of synthetic foam release hazardous chemicals, such as styrene and benzene, which are associated with carcinogenicity and other adverse health effects [5]. These drawbacks underscore the urgent need for alternatives that align with green and circular economy principles.

This is an open access article under the terms of the [Creative Commons Attribution](https://creativecommons.org/licenses/by/4.0/) License, which permits use, distribution and reproduction in any medium, provided the original work is properly cited.

© 2026 The Author(s). *CleanMat* published by Wiley-VCH GmbH.

Efforts to develop biodegradable foams derived from renewable resources have accelerated in recent years. Researchers have explored a variety of materials, including cellulose-based foams [6], foams derived from other natural sources, like pineapple [7], and biodegradable synthetic polymers [8]. Among biodegradable foams, mycelium-based foams have been introduced as a particularly promising solution, offering an eco-friendly approach to repurposing organic waste while addressing the environmental drawbacks of synthetic foams [9]. In this type of foam, mycelium, a vegetative part of fungi, is a crucial component, which spreads through the substrates during the fungal growth. Fungi can secrete enzymes that break down different fractions of lignocellulosic biomass and releasing nutrients for growth. Additionally, mycelium which is a network of branched hyphae acts as a natural adhesive binding the substrate particles together [4]. The production of mycelium-based foams typically relies on solid-state cultivation technique, where fungal growth takes place on solid substrates under low-moisture conditions. During this process, mycelium grows inside molds, taking on their shape and size [10, 11]. However, solid state cultivation faces challenges, including uneven distribution of mycelium, prolonged growth periods, and difficulties in process control [12]. Fungal cultivation can also be performed using submerged process, a method in which fungi are grown in a liquid medium under controlled conditions. This approach facilitates a uniform mycelial growth, efficient substrate utilization, and scalability for industrial production [13].

Following cultivation, the mycelium can be processed through homogenization and molding techniques via air drying or freeze-drying, to produce a porous foam structure. However, during air drying, the direct transition of water from liquid to gas generates capillary forces that often lead to pore shrinkage and structural collapse. In contrast, freeze-drying mitigates this issue by freezing the water within the pores, followed by reducing the pressure below the sublimation point. This process enables the water to transition directly from solid-state to gas without forming a liquid-vapor interface, thereby minimizing surface tension effects and preserving the structural integrity of the material, which results in formation of a porous foam structure [14].

Research on mycelium-based foam production has highlighted the versatility of substrates for fungal cultivation. These include cellulose-rich materials such as bleached softwood kraft pulp [15], and wood particles [16]; agro-industrial wastes such as bamboo sawdust, corn pericarp, rice hulls, and wheat straw [17, 18]. Mycelium-based foams are mostly developed using white-rot fungi belonging to basidiomycete filamentous fungal species including *Pleurotus ostreatus* [19] *Lentinus squarrosulus* [11] *Trametes versicolor*, and *Phanerochaete chrysosporium* [20].

The low density of mycelium-based foam is a major factor in their competitiveness, particularly for packaging applications. In addition to fungal strain, cultivation condition and substrate, post treatments such as pressing (cold or heated) significantly impact the final density of mycelium-based foams [21]. Mycelium-based foams exhibit ignition times comparable to extruded polystyrene (XPS). Compressive strength is another crucial property for evaluating mycelium-based foam as an alternative packaging

material. Variability in compressive strength is influenced by the substrate matrix and fungal species, with reported values ranging from 29 to 567 kPa, by Girometta et al. [21].

In this study, carrot pomace (CP), a by-product of the juice industry, was used as a substrate for the submerged cultivation of the filamentous fungus, *Aspergillus oryzae*. CP, rich in sugars, served as a nutrient source for fungal growth. The cellulosic fraction of CP was not consumed by the fungus and was harvested along with the fungal biomass from the bioreactor. The harvested materials were utilized to produce mycelium-based foams (MBF). The resulting MBF were analyzed for their physical, mechanical, and thermal properties to evaluate their viability as an alternative to conventional fossil-based foams.

2 | Material and Method

2.1 | Materials and Fungi Strain

Carrot pomace was generously supplied by Herrljunga Cider AB (Sweden) and was kept at -18°C until use. The study employed *Aspergillus oryzae* CBS 819.72 (Centraalbureau voor Schimmelcultures, Utrecht, The Netherlands). *A. oryzae* spores were grown on Potato Dextrose Agar (PDA) plates containing 4 g/L potato infusion, 20 g/L glucose, and 15 g/L agar. The plates were incubated at 30°C for 3–5 days and subsequently were sealed and stored at 4°C for future use.

2.2 | Fungal Biomass Production

2.2.1 | Preculture and Fungal Cultivation

Fungal cultivation was scaled up to a 26L bioreactor (Bioengineering, Wald, Switzerland) following successful cultivation of *A. oryzae* on bread waste [22]. The spore suspensions were prepared by adding 20 mL of sterile distilled water to the prepared agar plate and releasing the spores using an L-shaped cell spreader. The spore suspension was added to flasks containing 4% CP suspension (2 mL spore/100 mL CP suspension). The fungus was cultivated 24h at 35°C to prepare a pre-inoculum for seeding the 26L reactor.

The bioreactor was sterilized by steam injection at 130°C for 20 min. The substrate, 4wt% suspension of CP in water, was sterilized in an autoclave (Systec, Linden, Germany) at 121°C for 20 min. After cooling, the pre-inoculum was added to CP suspension, and the mixture was transferred to the sterile bioreactor in aseptic conditions. The cultivation process was conducted at 35°C for 72h without pH adjustment, maintaining an aeration rate of 2vvm (volume of air per volume of liquid per min). Afterward, the material comprising CP residue and fungal biomass was harvested from the bioreactor using a fabric polyester bag (210 μm , Reuseable BIAB bag) and compressed inside the bag using a mechanical press (screw press 121) to remove water, then washed and stored at -18°C until use.

2.2.2 | Analysis of Fungal Metabolites and Sugars

Monitoring the cultivation process is essential for controlling productivity and ensuring a high-quality output without contamination [23]. Liquid samples were collected from the bioreactor throughout the cultivation period to determine the concentrations of sugars and ethanol. The samples were centrifuged and filtered through 0.2 μm syringe filters to separate the liquid fraction prior to high-performance liquid chromatography (HPLC). Analysis was conducted using hydrogen-based ion-exchange column (Aminex HPX-87H; Bio-Rad, Hercules, CA, USA) at 60°C, with 0.6 mL/min of 5 mM H_2SO_4 as the eluent.

2.2.3 | Microscopy

The morphology of the harvested solids, containing the fungal biomass and CP residues, was analyzed using an ultrahigh-resolution field-emission scanning electron microscopy (FE-SEM, Hitachi S4800). Before SEM analysis, samples were collected during cultivation, frozen in liquid nitrogen to preserve their structural integrity, and subsequently lyophilized using a freeze-dryer (Labconco, Kansas City, MO, USA). Additionally, the cross-sectional structure of the mycelium-based foams was examined through imaging to evaluate their internal morphology.

2.3 | Development of MBF

The materials harvested from the bioreactors were autoclaved to deactivate the fungal cells. A 1wt% suspension of the harvested materials was then processed using a disk mill grinder machine (Super masscolloider, MKZA12-20J, Masuko Sangyo, Japan). The grinding process involved three, six, and nine cycles with standard silicon carbide grinding stones (MKE 46) at a rotational speed of 2700rpm. The gap between stones was adjusted to 50 μm (open gap). To produce MBF, the homogenized suspension containing mycelium and CP residues was poured into a plastic mold, frozen at -18°C , and then freeze-dried (Figure 1).

2.3.1 | Physical and Mechanical Characterizations of MBF

The moisture content of the MBF was determined by drying the foam in an oven at 105°C until a constant mass was achieved.

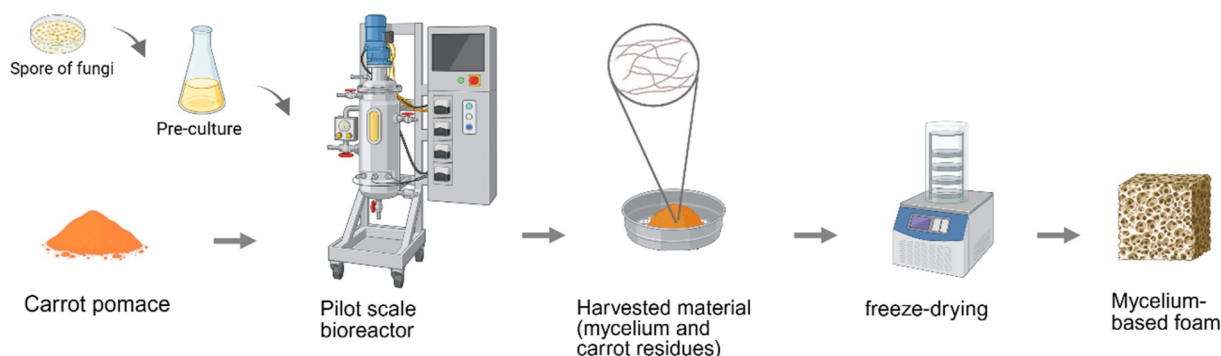


FIGURE 1 | Visual representation of the MBF development from CP (Created in Bio Render, <https://BioRender.com/1y88swp>).

The bulk density of MBF was calculated by dividing the mass of the foam by its volume (dimensions of the samples were recorded using a digital caliper by the measurements conducted in replicates). Specific Surface Area (SSA) and total pore volume of MBF was detected by Emmett Teller (BET) analysis (BELSORP Mini, Microtrac Bel, Osaka, Japan). Prior to measurement, the sample was first degassed under vacuum to a final pressure of 0.28 Pa. Nitrogen adsorption/desorption isotherms were then measured over a relative pressure range of (P/P_0) from 0.01 to 0.991. P is the actual pressure of nitrogen gas during the adsorption measurement and P_0 is saturation vapor pressure of nitrogen.

The compression test was performed according to EN 826:2013 standard, which is used for determining the compression behavior of thermal insulating products for building applications. The samples were conditioned for 24h prior to testing at 23°C and 50% relative humidity (RH). The test was conducted using a Zwick 100 tensile test machine (inv.nr BX32748) equipped with a load cell of 2.5 kN (Inv. Nr. BX32801). The test was executed with a deformation rate of 3 mm/min. The dimension of the sample was measured using a specific caliper (inv.nr BX61082). The forces at the respective deformations of 10%, 20% and 30% were recorded.

2.3.2 | Water Vapor Permeability (WVP) of MBF

The water vapor permeability (WVP) value represents the material's capacity to allow water vapor to permeate. The foam samples were sealed on top of containers filled with distilled water (100% relative humidity). These containers were placed in a desiccator containing silica gel at room temperature, creating a dry environment. The foam acted as a barrier between the high-humidity environment inside the container and the low-humidity environment in the desiccator. The initial mass of the foam-sealed containers was recorded, and subsequent mass measurements were taken at regular intervals. The mass reduction over time was attributed to the amount of water vapor transmitted through the foam. The rate of mass loss over time was determined using linear regression, and the WVP was calculated using the following formula:

$$\text{WVP} = \frac{\text{WVTR} * d}{\Delta P}$$

$$\text{WVTR} = \frac{\Delta m}{A * t}$$

Where WVTR represents the water vapor transmission rate (g/h. m²) and d denotes the thickness (m) of the foam. ΔP (Pa) signifies the water vapor pressure difference across the sample, which can be approximated based on the relative humidity difference between the container (approximately 100% RH) and the desiccator (approximately 0% RH). Δm represents the total weight loss, A is the area (m²) of the foam exposed to water vapor, and t (h) indicates the duration of the test.

2.3.3 | Biodegradability of MBF

A soil burial degradation test was conducted to evaluate the biodegradability of MBF in soil content at a depth of 10 cm under outdoor conditions at temperature ranging from -5°C to +6°C. After 40 days, the samples were collected, cleaned, and washed before drying in an oven at 50°C for 24h. The mass loss was calculated.

2.3.4 | Thermal Behavior of MBF

Thermal gravimetric analysis (TGA) was conducted to quantify the thermal stability of MBF using a Q500 TGA instrument (TA Instruments). MBF and commercial polyurethane foam, which is used as protective packaging, were heated from room temperature to 600°C at a heating rate of 10°C/min under a nitrogen atmosphere. The constant purge rate was maintained at 40 mL/min. Thermograms showing the percentage of weight loss against temperature were generated.

3 | Result and Discussion

3.1 | Fungal Cultivation in Bubble Column Bioreactor

In this study, *A. oryzae* was successfully cultivated on whole CP in a 26L bubble column reactor for 72h. At the end of cultivation, solids containing fungal biomass and CP residues were recovered (32.3 g/L). However, the accurate fungal biomass yield could not be determined due to the presence of CP particles. Throughout the cultivation, liquid samples were collected at 24, 48, and 72h to follow sugar consumption and metabolite formation. The fungal hyphae gradually expanded within the CP particles as illustrated in Figure 2c,d and e.

Notably, *A. oryzae* does not require external supplements or enzymatic pretreatment prior to submerged cultivation. The fungus produces a range of enzymes, including amylases, invertases, and glucosidases, which enable it to break down complex sugars into simpler forms for growth and energy production. As displayed in Figure 3, the initial concentration of glucose and sugar mix (other monomeric sugars such as xylose, fructose, galactose, and arabinose) in the reactor were 12.2 and 7.8 g/L respectively. After 24 h, the sugar levels decreased to 6.2 and 5.9 g/L. At the time of harvest (72h), sugar concentrations

had further reduced to respectively, 0.2 and 0.1 g/L, indicating nearly complete consumption of sugars by the fungus. This significant reduction confirmed that *A. oryzae* efficiently metabolizes free sugar during the growth phase. Despite sugar consumption, no ethanol was detected during cultivation which may be attributed to high aeration rate.

3.2 | Development of MBF

The material recovered from the bioreactor, composed of *A. oryzae* mycelium and CP, was subjected to different intensities of mechanical processing, including three, six, and nine grinding cycles. The ground suspensions were subsequently frozen and freeze-dried. Freeze drying, which enables the sublimation of frozen water directly from the solid phase to the gas phase, is particularly advantageous for producing advanced materials with interconnected porous structures [24]. Compared to conventional air-drying, freeze-drying is favorable method for preserving structural integrity of the materials [25].

Figure 4 illustrates the MBF which was initially molded in plastic cup and freeze dried (left image). A larger rectangular mold was used to make larger pieces of MBF (Figure 4, middle image) which were finally shaped into a prototype designed for cushioning packaging (Figure 4, right image), using a laboratory-scale, computer numerical control (CNC) cutting machine. The prototypes were strong enough to support and protect dry, light-weight products during handling and transportation.

3.2.1 | Physical Characterizations of MBF

The foam densities varied depending on the intensity and number of grinding cycles, with values of 21.6 ± 0.6 kg/m³ for three cycles (L-MBF), 21.2 ± 0.7 kg/m³ for six cycles (M-MBF), and 20.6 ± 0.8 kg/m³ for nine cycles (H-MBF) Statistical analysis confirmed that these differences were significant ($p < 0.05$) (Table 1). However, the reported densities of mycelium-based foam in the literature vary from 25 to 350 kg/m³ [26–28]. Notably, in most of these reports, solid-state cultivation was used. The foam densities observed here were slightly lower than those of polyurethane foam, a conventional plastic-based cushioning material that typically has densities ranging from 30 to 100 kg/m³ [28]. Figure 5 presents cross-sectional SEM images of the MBF produced using different grinding steps, showing a porous network composed of mycelium fibers with CP particles. In the foam made of unground material (Figure 5a), distinct mycelial structures were visible, remaining separate from the carrot particles. As the grinding intensity increased, the mycelium became homogenized and integrated more thoroughly with carrot particles due to physical engagement. However, no significant visual differences in foam structure were observed across different grinding cycles in the final foams, suggesting that while mechanical processing improves uniformity, it does not drastically alter the overall porous structure of MBF.

Brunauer-Emmett-Teller (BET) analysis was performed to determine the specific surface area (SSA) of the MBF samples. The SSA varied by changing the number of grinding cycles. The

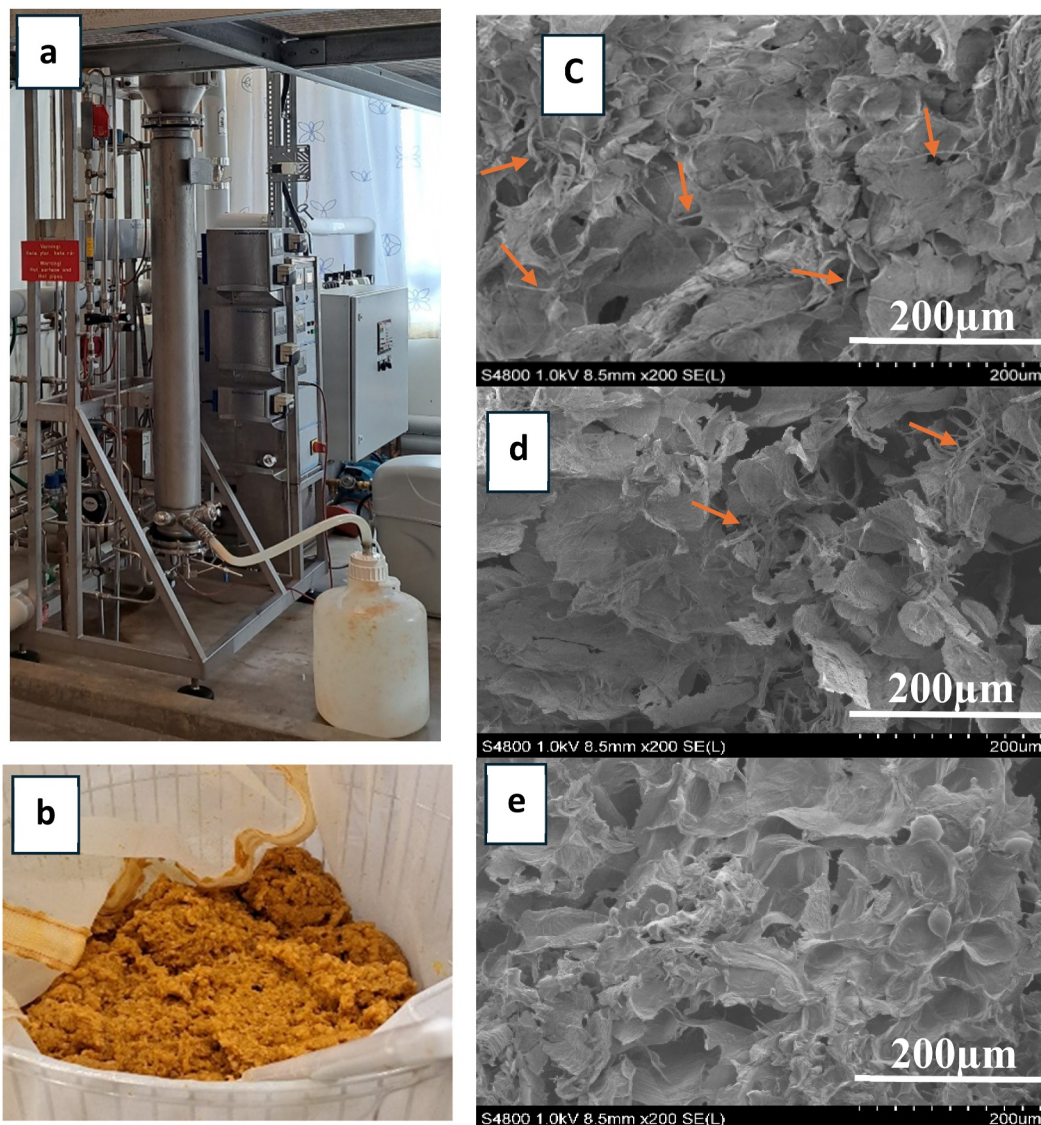


FIGURE 2 | (a) Fungal cultivation in a 26L bubble bioreactor; (b) Recovered materials from reactor; (c) microscopic images (FE-SEM) of freeze-dried recovered solids (mycelium of *A. oryzae* and CP particles) taken from the bioreactor after 24h, the orange arrows highlight the mycelium present in the carrot residue (d) 48h and (e) 72h of cultivation.

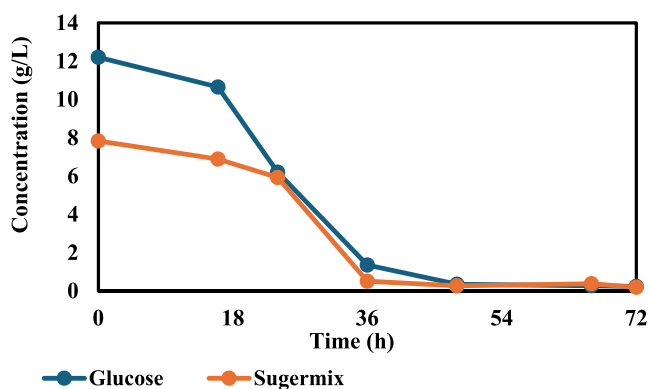


FIGURE 3 | Glucose and sugar mix concentration profiles during cultivation of *A. oryzae* in 26 L bioreactor.

sample subjected to three grinding cycles exhibited an SSA of 39.9 m²/g, which increased to 52.6 m²/g after six grinding cycles, likely due to better homogenization, the opening of

entanglements, and possible fibrillation of the particles. However, after nine grinding cycles, the SSA decreased to 36.4 m²/g, suggesting that excessive grinding led to particle fragmentation and formation of smaller segments that merged during the drying process, reducing the overall pore density. After nine grinding cycles, total pore volume increased to 0.34 cm³/g which was higher than the other cycles of grinding. This increase in pore volume may be due to structural changes that cause to the breakdown of pore walls, re-bonding and merging small pores, leading to the formation of larger macropores, which increase total pore volume but reduce SSA (since larger pores contribute less to SSA) [29].

In protective applications, materials with low SSA are often preferred due to their enhanced resistance to structural collapse under dynamic loads. This characteristic makes them suitable for applications requiring repeated or prolonged stress resistance such as protective padding or foam used in structural components. Conversely, materials exhibiting high SSA and extensive



FIGURE 4 | MBF that are molded in cylinder and cubic and its prototype as cushioning packaging.

TABLE 1 | Physical and mechanical properties of MBF's are composed of *A. oryzae* and CP particles.

Number of grinding cycles	Density (kg/m ³)	Specific surface area (m ² /g)	Total pore volume (cm ³ /g)	WVP (g.mm/kPa.h.m ²)	Compression stress in cyclical loading (KPa)		
					10%	20%	30%
L-MBF	21.6 ± 0.6	39.9	0.16	31.9 ± 0.3	6.3 ± 0.0	13.2 ± 0.6	18.3 ± 1.2
M-MBF	21.2 ± 0.7	52.6	0.19	31.7 ± 0.3	5.9 ± 0.4	15.1 ± 0.5	21.7 ± 0.9
H-MBF	20.6 ± 0.8	36.4	0.34	31.1 ± 0.6	5.2 ± 0.7	14.0 ± 1.7	21.4 ± 2.3

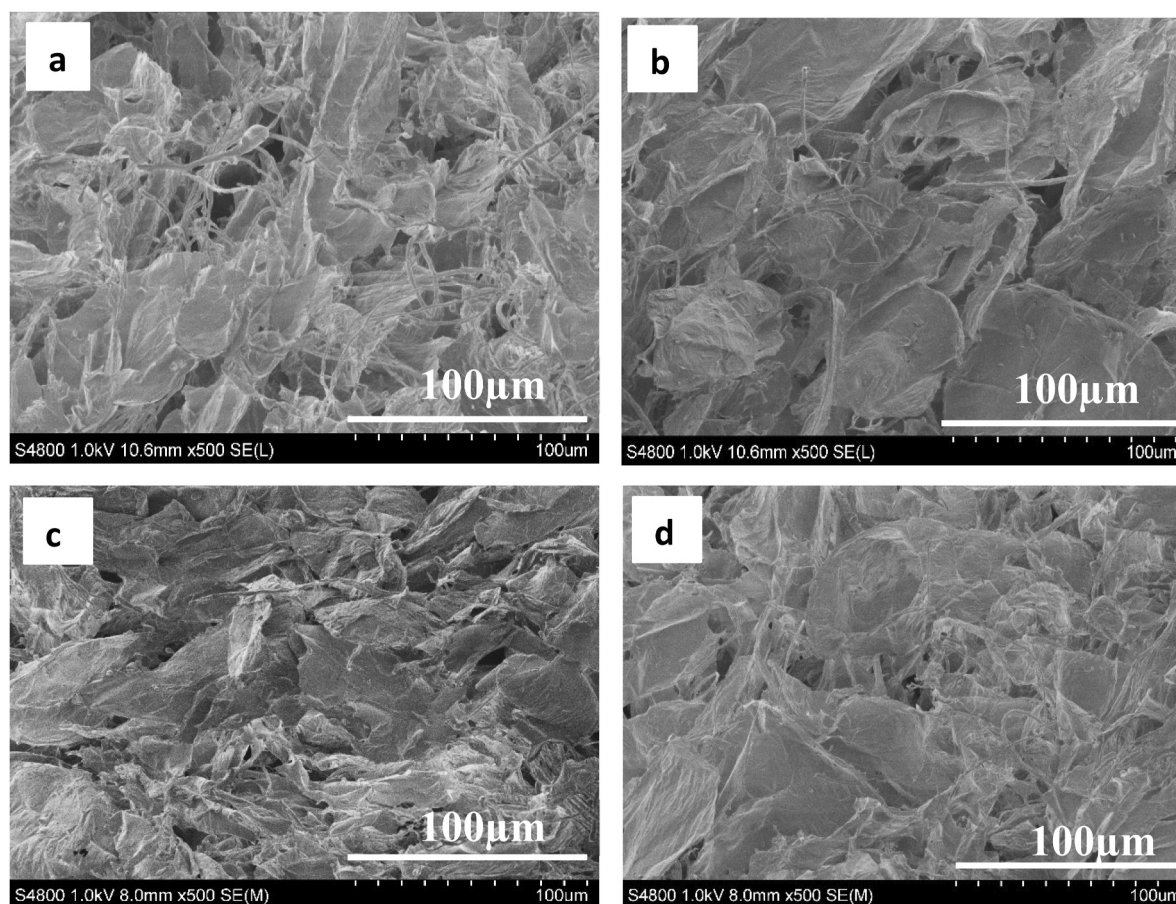


FIGURE 5 | Cross-section SEM images of mycelium-based foam made from (a) non-grind materials (b) after 3 cycles of grinding (L-MBF) (c) after 6 cycles of grinding (M-MBF) and (d) after 9 cycles of grinding (H-MBF).

porosity are more appropriate for vibration damping, as their microporous network facilitates energy absorption. Zhao et al. [30] reported that ultrafine grinding of spent mushroom substrate (SMS) resulted in an SSA values of 4.4 m²/g for the foam, while the

foam's density was measured as 0.09 ± 0.01 kg/m³. According to Ferraia et al. [31], the SSA value for cellulose-based lightweight foams in the literature vary widely, ranging from 1 to 633 m²/g with a density of 9–220 kg/m³. This variation could also be

influenced by fabrication processes, such as templating and drying, that affect the final structure.

Water vapor permeability (WVP) is a key property that determines a material's ability to resist the transmission of water vapor. This characteristic is essential for maintaining the structural integrity and performance of packaging materials, as excessive moisture can reduce material strength and efficiency. In this study, the WVP value for all three foam types were similar, around 31 g.mm/kPa.h.m², indicating a moderate resistance to moisture transmission. Lower WVP is generally preferred for protective applications to minimize water vapor penetration and maintain structural stability. For qualitative reference, the water vapor permeability of sheets produced from spent mushroom substrate (SMS) was reported 50 and 41g.h⁻¹. m⁻² at 90 RH% [30]. However, direct numerical comparison is limited because these values were reported as WVTR rather than WVP and were obtained under different experimental conditions.

3.2.2 | Compression—Stress of MBF

In packaging products, compressive strength is an essential parameter for evaluating a material's resilience and protective capability, as it determines how effectively the packaging can safeguard its contents [15]. The compression test results provided insights into the mechanical behavior of MBF under cyclic loading and varying levels of deformation (10%, 20%, and 30%). Observations also revealed that the compressed MBF began to collapse under compression, as illustrated in Figure 6.

The compression test demonstrated a strain-dependent response in the compressive behavior of the MBF. At 10% deformation, the compressive stress was 6.3, 5.9 and 5.20 kPa for L-MBF, M-MBF and H-MBF, respectively. A statistically significant difference in the compressive stress ($p < 0.05$) was observed between different MBF. However, as the strain increases, these differences

diminished and at 20% and 30% deformation, compressive stress ranged from 13.2 to 15.1 kPa and 18.3–21.7 kPa, respectively. The differences at these levels were not statistically significant ($p > 0.05$), indicating that different MBF exhibited converging compressive performance at higher deformation. This increase in compressive stress with deformation can be attributed to the densification effect, where the porous structure of MBF gradually collapses under compression, leading to higher resistance against further deformation [32]. This strain-dependent response provides valuable design considerations for packaging applications, where MBF must protect goods while maintaining their structural integrity under varying levels of compression.

Mycelium-based materials have demonstrated a broad range of mechanical strengths, depending on their density and composition. For instance, a mycelium foam with a density of 320 kg/cm³ achieved a compressive strength of approximately 1300 kPa [5]. Tacer-Caba et al. [33] developed biofoams with a density of 516 kg/m³, which demonstrated compressive strength of 274.8 kPa. This variation in compressive strength suggests that MBF can be tailored for specific applications by adjusting the density and structural composition.

Moreover, Womer et al. [34] highlighted that MBF without reinforcement exhibit compressive strengths ranging from 1 to 1029 kPa, based on substrate and strain, whereas hybridized mycelium foams, when combined with raw cellulose, achieved higher compressive strength range of 25–160 kPa. Conventional materials, such as expanded polystyrene (EPS) and extruded polystyrene (XPS), demonstrated compressive strengths 60–400 kPa with densities between 12 and 48 kg/m³ [34]. Polyurethane foam, a common material used in packaging and insulation, also displayed compression strengths between 180 and 300 kPa, with densities ranging from 36 to 103 kg/m³ [35].

Ashby's bubble chart is a graphical tool used to visually evaluate the positioning of produced materials in comparison to commercially available foam materials for specific applications.

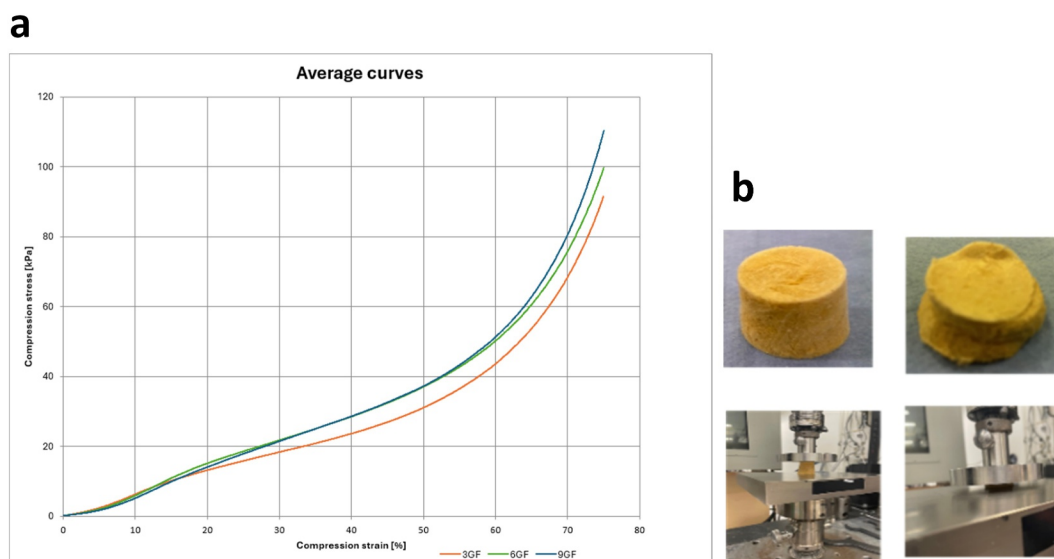


FIGURE 6 | (a) Average compression stress–strain curves, where 3, 6, and 9 GF indicate the low, medium and high grinding cycles used in production of MBF (b) MBF subjected to a compression test.

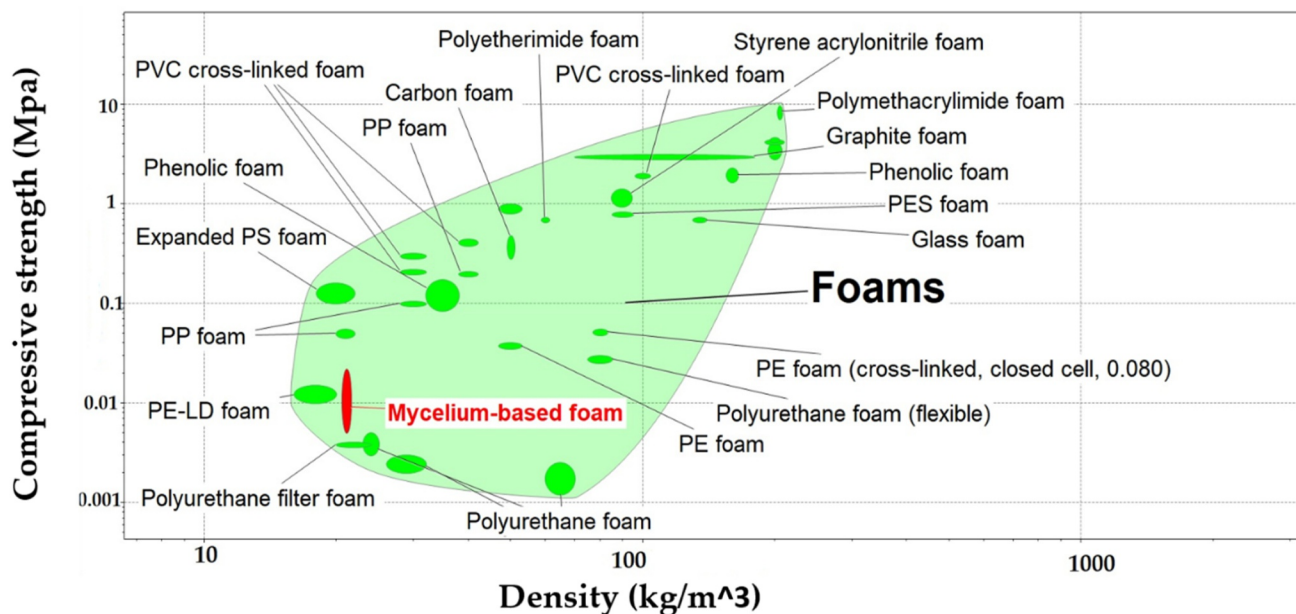


FIGURE 7 | A material property, plotting density against compression strength for mycelium-based foam on Ashby's chart for foam materials (reproduced the chart created using CES Edupack 2021, ANSYS Granta 2021 Granta Design).

It provides insights into their suitability based on mechanical and physical properties. In this study, the Ashby plot includes a red bubble representing the investigated mycelium-based foams (MBFs), while the green bubbles correspond to commercial foams such as polyethylene low-density foam (PE-LD) and polyurethane foam (Figure 7). The chart indicates that MBFs exhibit physical and mechanical behaviors comparable to those of commercial foam materials, particularly in terms of lightweight characteristics and cushioning capability. However, it also highlights that MBF are not yet viable substitutes for rigid foams. This suggests that while MBF may not be suitable for load-bearing applications, they are well-suited for cushioning, shock absorption, and protective packaging. Furthermore, their potential as a biodegradable alternative makes them particularly advantageous for environmentally friendly solutions, especially for transport packaging applications. Similarly, Appels et al. [35] categorized non-pressed mycelium composites produced using *Trametes multicolor* and *Pleurotus ostreatus* cultivated on beech sawdust, rapeseed straw, and cotton fiber substrates under solid state cultivation, within the foam bubble classification based on their flexural modulus and density. Additionally, applying the cold and hot press resulted in slight modification to their foam-like properties.

3.2.3 | Thermal Behavior of MBF

The thermal stability and decomposition behavior of the MBF were analyzed using thermogravimetric analysis (TGA), as shown in Figure 8. The results indicate that MBF exhibits thermal degradation similar to most cellulosic-derived materials. Derivative thermogravimetric (DTG) analysis of MBF exhibited the initial mass loss of 7.4% occurring between 50°C and 200°C, due to evaporation of water and volatile compounds, before the thermal decomposition of cellulose and mycelium.

According to Zange et al. reported [36], fungus converts the substrate into lower molecular weight compounds, making them more volatile during heating. The next stage of degradation occurs between 200°C and 350°C, corresponding to the decomposition of hemicellulose and other organic constituents present in the CP residues and mycelium. This phase accounts for the major mass loss (62.6%) of MBF. A subsequent degradation peak was observed at approximately 350°C–400°C, with a mass loss of 24%, attributed to the decomposition of cellulose and other structural biopolymers [5, 20]. In the final stage, occurring between 400°C and 600°C, the primary residual char degrades to form carbonaceous char residue [37].

TGA of the MBF was also compared with that of polyurethane foam. The results highlight distinct differences in thermal stability and degradation behavior, which reflect differences in their compositions and structural properties. Polyurethane foam exhibits a sharper degradation profile involving multiple stages. Initially, the breakdown of urethane linkages occurred, followed by the degradation of the polyol segments [38]. Overall, the thermal analysis demonstrates that while polyurethane foam exhibits higher thermal stability, as evidenced by its resistance to initial degradation, mycelium-based foam offers unique advantages in terms of char formation. This char layer acts as an insulating barrier, limiting heat transfer and oxygen diffusion [21, 39].

3.2.4 | Soil Burial Test

The biodegradability of mycelium foam was evaluated using a soil burial degradation test. Specimens were buried approximately 10 cm below the surface in the garden area of the department building, where they were exposed to natural environmental conditions, without any control over moisture

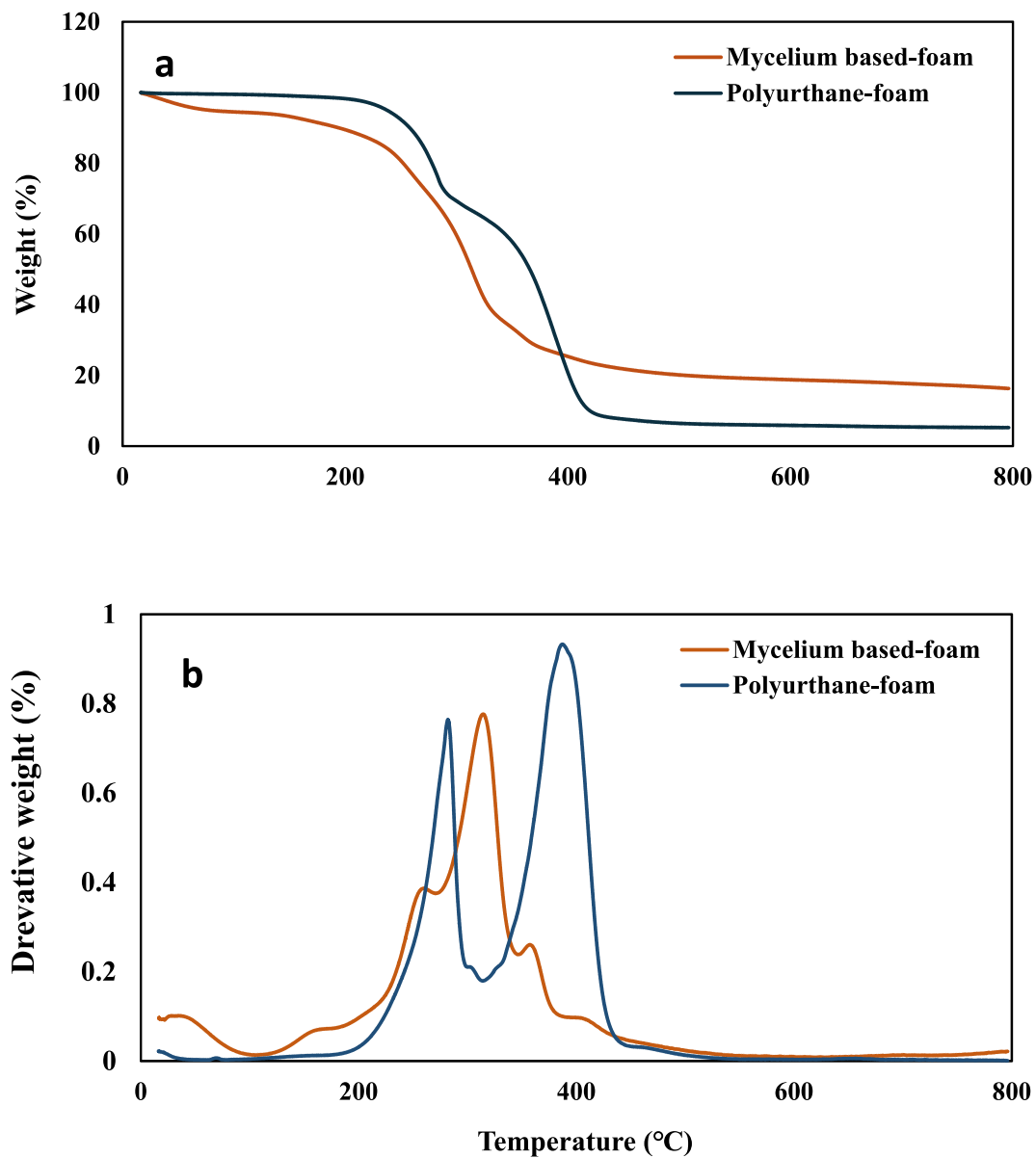


FIGURE 8 | (a) Thermogravimetric analysis and (b) derivative thermogravimetric analysis of MBF and polyurethane as plastic-based foam.



FIGURE 9 | Biodegradability test, including soil burial degradation test of the MBF after 40 days.

levels or temperature. Throughout the test period, the temperatures fluctuated between -5 and $+6^{\circ}\text{C}$. The mycelium foam exhibited a significant mass reduction of approximately 50%–70%, indicating active biodegradation facilitated by soil microorganisms and moisture. After 40 days, only a small

portion of the initial mass was retained. Figure 9 illustrates the degradation behavior of the mycelium foam during soil burial. Farrahnoor et al. [40] also assessed the degradation rate of the mycelium-based composite produced by cultivating fungi on kenaf as substrate through a similar soil burial experiment.

Their findings demonstrated that by day 14, the samples had decomposed into powdery fibers resulting in 100% weight loss. Mycelium composites can achieve substantial biodegradation, however this process depends on the microbial activity of soil type, temperature and substrate composition [41].

4 | Conclusion

Mycelium-based foam presents a promising alternative to lightweight synthetic foams. The process for development of MBF in this study included submerged cultivation of the fungus in carrot pomace which offers advantages such as waste management and scalability. Sugar consumption and SEM microscopy, confirming the mycelium growth. The MBF exhibited an average density of 21.1 kg/m³ and demonstrated a compressive resistance of 20.5 kPa when compressed to 30% of its original thickness. According to the Ashby chart, MBF are comparable to commercial lightweight foams, making them suitable for protective and cushioning applications.

Author Contributions

S. Najmeh Mousavi: conceptualization, data curation, formal analysis, investigation, methodology, writing – original draft preparation. **Paula Pou I Rodríguez:** investigation. **Juliana Aristéia de Lima:** investigation. **E. R. Kanishka B. Wijayarathna:** investigation. **Sunil Kumar Ramamoorthy:** conceptualization, validation, review and editing. **Minna Hakkarainen:** validation, review and editing. **Akram Zamani:** conceptualization, supervision, project administration, review and editing.

Acknowledgments

Special thanks to Magnus Götlind for design of the prototype by CNC machine and Peter Widén in RISE institute for performing the compression tests. The authors also thank Zeinab Qazanfarzadeh for providing the graphical abstract.

Funding

The work was financed by Vinnova, project number 2021-03726.

Ethics Statement

The fungal strains an *Aspergillus oryzae* was obtained from Centraalbureau voor Schimmelcultures, Utrecht in Netherlands. These strains are categorized as biosafety level 1, and there was no need for ethical approval for their use in the study.

Conflicts of Interest

The authors declare no conflicts of interest.

Data Availability Statement

The data that supports the findings of this study are available within the article.

References

1. T. Suwandecha and S. Pisuchpen, Characterization and Performance Evaluation of Mycelium-Based Biofoams for Cushioning Materials Using Edible Mushrooms, (2024).

2. AgileIntel Research (ChemIntel360). Market Volume of Polyurethane Worldwide From 2015 to 2022, With a Forecast for 2023 to 2030, https://www.statista.com/statistics/720341/global-polyurethane-market-size-forecast/?utm_source=chatgpt.com.
3. GlobalData. Production Capacity of Polystyrene Worldwide in 2022 and 2026, https://www.statista.com/statistics/1065889/global-polystyrene-production-capacity/?utm_source=chatgpt.com.
4. K. B. Bonga, L. Bertolacci, M. Contardi, et al., “Mycelium Agrowaste-Bound Biocomposites as Thermal and Acoustic Insulation Materials in Building Construction,” *Macromolecular Materials and Engineering* 309, no. 6 (2024): 2300449, <https://doi.org/10.1002/mame.202300449>.
5. C. Bruscato, E. Malvessi, R. N. Brandalise, and M. Camassola, “High Performance of Macrofungi in the Production of Mycelium-Based Biofoams Using Sawdust—Sustainable Technology for Waste Reduction,” *Journal of Cleaner Production* 234 (2019): 225–232, <https://doi.org/10.1016/j.jclepro.2019.06.150>.
6. M. Reichler, S. Rabensteiner, L. Törnblom, et al., “Scalable Method for Bio-Based Solid Foams That Mimic Wood,” *Scientific Reports* 11, no. 1 (2021): 24306, <https://doi.org/10.1038/s41598-021-03764-0>.
7. A. Namphonsane, T. Amornsakchai, C. H. Chia, et al., “Development of Biodegradable Rigid Foams From Pineapple Field Waste,” *Polymers* 15, no. 13 (2023): 2895, <https://doi.org/10.3390/polym15132895>.
8. H. Yang, G. Xu, J. Li, et al., “Fabrication of Bio-Based Biodegradable Poly (Lactic Acid)(PlA) and Poly (3-Hydroxybutyrate-co-3-Hydroxyvalerate) (PHBV) Composite Foams for Highly Efficient Oil-Water Separation,” *International Journal of Biological Macromolecules* 257 (2024): 128750, <https://doi.org/10.1016/j.ijbiomac.2023.128750>.
9. N. M. Majib, N. D. Yaacob, S. S. Ting, et al., “Fungal Mycelium-Based Biofoam Composite: A Review in Growth, Properties and Application,” *Progress in Rubber, Plastics and Recycling Technology* 41, no. 1 (2025): 91–123, <https://doi.org/10.1177/14777606241252702>.
10. N. I. Nashiruddin, K. S. Chua, A. F. Mansor, et al., “Effect of Growth Factors on the Production of Mycelium-Based Biofoam,” *Clean Technologies and Environmental Policy* 24, no. 1 (2022): 351–361, <https://doi.org/10.1007/s10098-021-02146-4>.
11. T. Suwandecha and S. Pisuchpen, “Characterization and Performance Evaluation of Mycelium-Based Biofoams for Cushioning Materials Using Edible Mushrooms,” *Journal of Renewable Materials* 12, no. 11 (2024): 1811–1836, <https://doi.org/10.32604/jrm.2024.056334>.
12. A. Cerda, A. Artola, R. Barrena, X. Font, T. Gea, and A. Sánchez, “Innovative Production of Bioproducts From Organic Waste Through Solid-State Fermentation,” *Frontiers in Sustainable Food Systems* 3 (2019): 63, <https://doi.org/10.3389/fsufs.2019.00063>.
13. V. Whabi, B. Yu, and J. Xu, “From Nature to Design: Tailoring Pure Mycelial Materials for the Needs of Tomorrow,” *Journal of Fungi* 10, no. 3 (2024): 183, <https://doi.org/10.3390/jof10030183>.
14. Y. Sun, Y. Chu, W. Wu, and H. Xiao, “Nanocellulose-Based Lightweight Porous Materials: A Review,” *Carbohydrate Polymers* 255 (2021): 117489, <https://doi.org/10.1016/j.carbpol.2020.117489>.
15. H. Ahmadi, A. O’Keefe, M. A. Bilek, et al., “Investigation of Properties and Applications of Cellulose-Mycelium Foam,” *Journal of Materials Science* 57, no. 22 (2022): 10167–10178, <https://doi.org/10.1007/s10853-022-07302-9>.
16. W. Sun, M. Tajvidi, C. Howell, and C. G. Hunt, “Insight Into Mycelium-Lignocellulosic Bio-Composites: Essential Factors and Properties,” *Composites Part A: Applied Science and Manufacturing* 161 (2022): 107125, <https://doi.org/10.1016/j.compositesa.2022.107125>.
17. M. A. Shakir and M. I. Ahmad, “Bioproduct Advances: Insight Into Failure Factors in Mycelium Composite Fabrication,” *Biofuels, Bioproducts and Biorefining* (2024), <https://doi.org/10.1002/bbb.2620>.
18. W. Aiduang, K. Jatuwong, P. Jinanukul, et al., “Sustainable Innovation: Fabrication and Characterization of Mycelium-Based Green

- Composites for Modern Interior Materials Using Agro-Industrial Wastes and Different Species of Fungi,” *Polymers* 16, no. 4 (2024): 550, <https://doi.org/10.3390/polym16040550>.
19. M. M. Aranda-Calipuy, A. Roncal-Lázaro, M. A. Quezada-Alvarez, et al., “Pleurotus ostreatus Mycelium and Sugarcane Bagasse as Substitute Environment-Friendly Material for Polystyrene Foam,” *Sustainability* 15, no. 12 (2023): 9157, <https://doi.org/10.3390/su15129157>.
20. M. Zhang, J. Xue, R. Zhang, et al., “Mycelium Composite With Hierarchical Porous Structure for Thermal Management,” *Small* 19, no. 46 (2023): 2302827, <https://doi.org/10.1002/sml.202302827>.
21. C. Girometta, A. M. Picco, R. M. Baiguera, et al., “Physico-Mechanical and Thermodynamic Properties of Mycelium-Based Composites: A Review,” *Sustainability* 11, no. 1 (2019): 281, <https://doi.org/10.3390/su11010281>.
22. S. E. Svensson, E. K. B. Wijayarathna, N. K. Kalita, M. Hakkarainen, and A. Zamani, “Development of Hydrogels From Cell Wall of *Aspergillus oryzae* Containing Chitin-Glucan and Wet Spinning to Monofilaments,” *International Journal of Biological Macromolecules* 278 (2024): 134285, <https://doi.org/10.1016/j.ijbiomac.2024.134285>.
23. N. Rousta, C. Hellwig, S. Wainaina, et al., “Filamentous Fungus *Aspergillus Oryzae* for Food: From Submerged Cultivation to Fungal Burgers and Their Sensory evaluation—A Pilot Study,” *Foods* 10, no. 11 (2021): 2774, <https://doi.org/10.3390/foods10112774>.
24. M. M. Mehanna and K. K. Abba, “Recent Advances in Freeze-Drying: Variables, Cycle Optimization, and Innovative Techniques,” *Pharmaceutical Development and Technology* 27, no. 8 (2022): 904–923, <https://doi.org/10.1080/10837450.2022.2129385>.
25. K. R. Ward and P. Matejtschuk, *The Principles of freeze-drying and Application of Analytical Technologies* (Cryopreservation and freeze-drying protocols, 2021), 99–127.
26. J. A. López Nava, J. Méndez González, X. Ruelas Chacón, and J. A. Nájera Luna, “Assessment of Edible Fungi and Films Bio-Based Material Simulating Expanded Polystyrene,” *Materials and Manufacturing Processes* 31, no. 8 (2016): 1085–1090, <https://doi.org/10.1080/10426914.2015.1070420>.
27. K. Tanner, L. S. Chatman, and D. Allen, “Approaches to Cell Biology Teaching: Cooperative Learning in the Science Classroom—Beyond Students Working in Groups,” *Cell Biology Education* 2, no. 1 (2003): 1–5, <https://doi.org/10.1187/cbe.03-03-0010>.
28. W. Aiduang, K. Jatuwong, T. Luangharn, et al., “A Review Delving Into the Factors Influencing Mycelium-Based Green Composites (MBCs) Production and Their Properties for Long-Term Sustainability Targets,” *Biomimetics* 9, no. 6 (2024): 337, <https://doi.org/10.3390/biomimetics9060337>.
29. C. Zhang, M. Wu, S. Yang, X. Song, and Y. Xu, “Combined Mechanical Grinding and Enzyme Post-Treatment Leading to Increased Yield and Size Uniformity of Cellulose Nanofibrils,” *Cellulose* 27, no. 13 (2020): 7447–7461, <https://doi.org/10.1007/s10570-020-03335-y>.
30. A. Zhao, L. Berglund, L. Rosenstock Völtz, et al., “Fungal Innovation: Harnessing Mushrooms for Production of Sustainable Functional Materials,” *Advanced Functional Materials* 35, no. 2 (2024): 2412753, <https://doi.org/10.1002/adfm.202412753>.
31. E. S. Ferreira, C. A. Rezende, and E. D. Cranston, “Fundamentals of Cellulose Lightweight Materials: Bio-Based Assemblies With Tailored Properties,” *Green Chemistry* 23, no. 10 (2021): 3542–3568, <https://doi.org/10.1039/d1gc00326g>.
32. A. Rigobello and P. Ayres, “Compressive Behaviour of Anisotropic Mycelium-Based Composites,” *Scientific Reports* 12, no. 1 (2022): 6846, <https://doi.org/10.1038/s41598-022-10930-5>.
33. Z. Tacer-Caba, J. J. Varis, P. Lankinen, and K. S. Mikkonen, “Comparison of Novel Fungal Mycelia Strains and Sustainable Growth Substrates to Produce Humidity-Resistant Biocomposites,” *Materials & Design* 192 (2020): 108728, <https://doi.org/10.1016/j.matdes.2020.108728>.
34. S. Womer, T. Huynh, and S. John, “Hybridizations and Reinforcements in Mycelium Composites: A Review,” *Bioresource Technology Reports* 22 (2023): 101456, <https://doi.org/10.1016/j.biteb.2023.101456>.
35. F. V. W. Appels, S. Camere, M. Montalti, et al., “Fabrication Factors Influencing Mechanical, Moisture- and Water-Related Properties of Mycelium-Based Composites,” *Materials & Design* 161 (2019): 64–71, <https://doi.org/10.1016/j.matdes.2018.11.027>.
36. M. Zhang, Z. Zhang, R. Zhang, Y. Peng, M. Wang, and J. Cao, “Lightweight, Thermal Insulation, Hydrophobic Mycelium Composites With Hierarchical Porous Structure: Design, Manufacture and Applications,” *Composites Part B: Engineering* 266 (2023): 111003, <https://doi.org/10.1016/j.compositesb.2023.111003>.
37. M. Jones, K. Weiland, M. Kujundzic, et al., “Sustainable Mycelium-Derived Chitinous Thin Films,” in *22nd International Conference on Composite Materials (ICCM22)*, (2019).
38. L. Jiao, H. Xiao, Q. Wang, and J. Sun, “Thermal Degradation Characteristics of Rigid Polyurethane Foam and the Volatile Products Analysis With TG-FTIR-MS,” *Polymer Degradation and Stability* 98, no. 12 (2013): 2687–2696, <https://doi.org/10.1016/j.polymdegradstab.2013.09.032>.
39. M. Jones, T. Bhat, E. Kandare, et al., “Thermal Degradation and Fire Properties of Fungal Mycelium and Mycelium - Biomass Composite Materials,” *Scientific Reports* 8, no. 1 (2018): 17583, <https://doi.org/10.1038/s41598-018-36032-9>.
40. A. Farrahnoor, N. A. A. Sazali, H. Yusoff, and B. T. Zhou, “Effect of Beeswax and Coconut Oil as Natural Coating Agents on Morphological, Degradation Behaviour, and Water Barrier Properties of Mycelium-based Composite in Modified Controlled Environment,” *Progress in Organic Coatings* 196 (2024): 108763, <https://doi.org/10.1016/j.porgcoat.2024.108763>.
41. S. Kalka, T. Huber, J. Steinberg, K. Baronian, J. Müssig, and M. P. Staiger, “Biodegradability of All-Cellulose Composite Laminates,” *Composites Part A: Applied Science and Manufacturing* 59 (2014): 37–44, <https://doi.org/10.1016/j.compositesa.2013.12.012>.